Developmental Cell
Short Article

Selective Autophagy Regulates Insertional Mutagenesis by the Ty1 Retrotransposon in *Saccharomyces cerevisiae*

Kuninori Suzuki,[1,*] Mayumi Morimoto,[1] Chika Kondo,[1] and Yoshinori Ohsumi[1,*]
[1]Frontier Research Center, Tokyo Institute of Technology, 4259-S2-12 Nagatsuta-cho, Midori-ku, Yokohama 226-8503, Japan
*Correspondence: kuninori@iri.titech.ac.jp (K.S.), yohsumi@iri.titech.ac.jp (Y.O.)
DOI 10.1016/j.devcel.2011.06.023

SUMMARY

Macroautophagy (autophagy) is a bulk degradation system for cytoplasmic components and is ubiquitously found in eukaryotic cells. Autophagy is induced under starvation conditions and plays a cytoprotective role by degrading unwanted cytoplasmic materials. The Ty1 transposon, a member of the Ty1/*copia* superfamily, is the most abundant retrotransposon in the yeast *Saccharomyces cerevisiae* and acts to introduce mutations in the host genome via Ty1 virus-like particles (VLPs) localized in the cytoplasm. Here we show that selective autophagy downregulates Ty1 transposition by eliminating Ty1 VLPs from the cytoplasm under nutrient-limited conditions. Ty1 VLPs are targeted to autophagosomes by an interaction with Atg19. We propose that selective autophagy safeguards genome integrity against excessive insertional mutagenesis caused during nutrient starvation by transposable elements in eukaryotic cells.

INTRODUCTION

Transposable elements comprise a considerable fraction of eukaryotic genomes; for example, they occupy about half of the human genome and ~70% of the genomes of some plant species (Feschotte et al., 2002; Lander et al., 2001). Transposons are able to modulate gene expression and promote genome evolution by introducing mutations into their host genomes through their mobility and recombination (Gogvadze and Buzdin, 2009; Volff, 2006). Retrotransposons, a class of transposable elements, are transcribed to RNA intermediates, which are used as templates for reverse transcription back to DNA, and then the cDNA copies are integrated within host genomes. Interestingly, retrotransposons resemble retroviruses in their structure and life cycle except they are not infectious.

Ty1 is the most abundant retrotransposon in the yeast *Saccharomyces cerevisiae*, which is frequently used as a model system to investigate the life cycle of retrotransposons. Translation of Ty1 mRNA results in the synthesis of two primary products: Ty1 Gag-p49 and Ty1 Gag-Pol-p199 (Voytas and Boeke, 2002). Ty1 Gag-p49 is proteolytically processed at the C terminus to produce Ty1 Gag-p45, a mature capsid protein (Merkulov et al., 1996). Ty1 Gag-p49 and Ty1 Gag-p45 comprise Ty1 virus-like particles (VLPs), where Ty1 mRNAs are reverse transcribed into cDNA. Ty1 VLPs form a large cluster in the cytoplasm when Ty1 elements are overexpressed (Garfinkel et al., 1985). A recent study using fluorescence microscopy has shown that Ty1 Gag and Ty1 mRNAs colocalize at cytoplasmic foci (Checkley et al., 2010).

Autophagy is a bulk degradation system of cytoplasmic constituents induced under starvation conditions (Suzuki and Ohsumi, 2007). In yeast, vacuolar aminopeptidase I (Ape1) is synthesized as a proform (prApe1) and processed into mature Ape1 (mApe1) in the vacuole (Klionsky et al., 1992). After synthesis, prApe1 travels to the cytoplasm-to-vacuole targeting (Cvt) complex. The Cvt complex is defined by electron microscopy as an electron-dense core structure of prApe1 (Ape1 complex) accompanied by several surrounding particles (Baba et al., 1997). Under a fluorescence microscope, the Ape1 complex appears as a dot-like structure next to the vacuole (Shintani et al., 2002; Suzuki et al., 2002).

The Cvt complex is transported to the vacuole by Cvt vesicles under nutrient-rich conditions and by autophagosomes during starvation conditions (Baba et al., 1997). Cvt vesicles are basically responsible for the biosynthesis of mApe1, whereas most cytoplasmic material in autophagosomes is destined to be degraded in the vacuole. Eventually, these degradation products are used as building blocks necessary for biosynthesis to survive under starvation conditions (Onodera and Ohsumi, 2005). In this study, we find that the Ty1 VLP is selectively transported to the vacuole in an Atg19-dependent manner. Under starvation conditions, the Ty1 transposition is downregulated by selective autophagy.

RESULTS AND DISCUSSION

Surrounding Particles of the Cvt Complex Are Identified as the Ty1 Virus-Like Particles

Composed of the Ape1 complex and surrounding particles, the Cvt complex is selectively transported to the vacuole by Cvt vesicles/autophagosomes (Baba et al., 1997). Identifying the nature of these particles has been a long-standing challenge. Fluorescence microscopic analyses have shown that the Ape1 complex is localized next to the vacuole as a dot-like structure (Shintani et al., 2002; Suzuki et al., 2002). Furthermore, a recent study demonstrated the colocalization of Ty1 Gag and Ty1

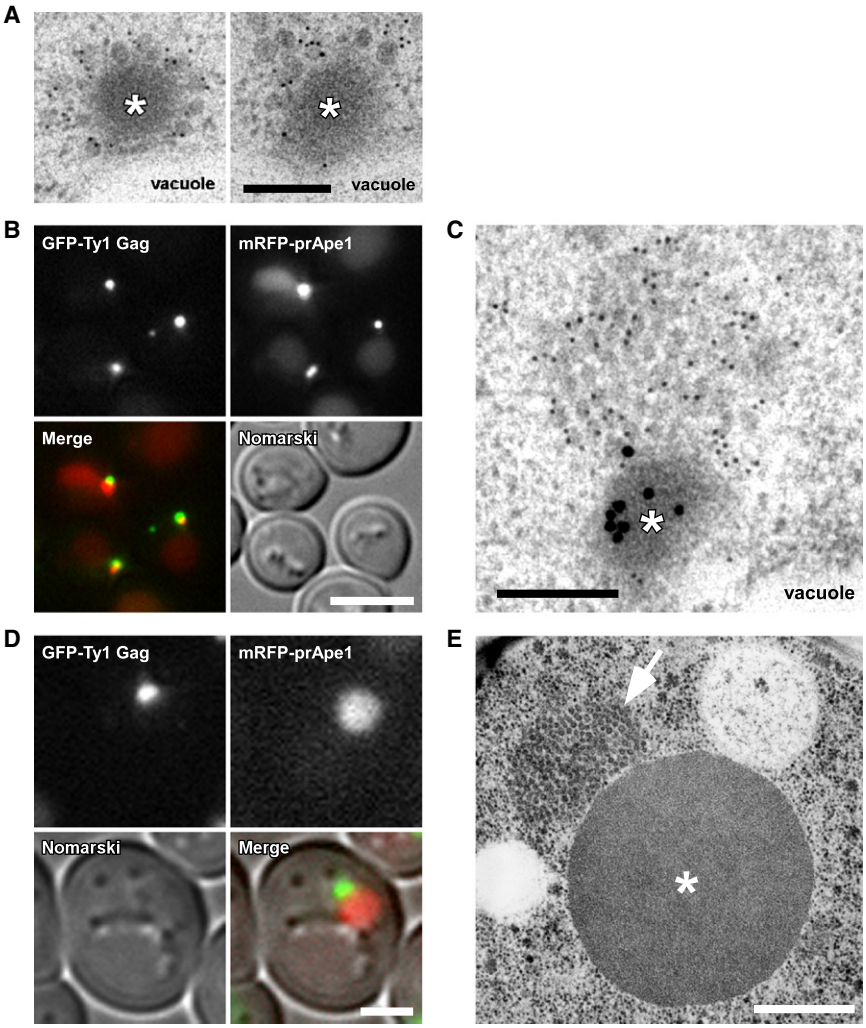

Figure 1. Surrounding Particles of the Cvt Complex Are Identified as the Ty1 VLPs

(A) Endogenous Ty1 VLPs are detected by immunoelectron microscopy with anti-Ty1 Gag antibodies. *atg1*Δ cells treated with rapamycin for 3 hr were subjected to immunoelectron microscopy. Asterisks indicate Ape1 complexes. Scale bar represents 200 nm.

(B) Localization of Ty1 VLPs and the Ape1 complex. mRFP-prApe1 cells overexpressing GFP-Ty1 Gag were treated with rapamycin for 6 hr. Scale bar represents 5 μm.

(C) Immunoelectron microscopy with anti-Ty1 Gag antibodies and anti-Ape1 antiserum. *atg1*Δ cells overexpressing GFP-Ty1 Gag were treated with rapamycin for 4 hr. Ty1 Gag and prApe1 were labeled with 10-nm and 20-nm colloidal gold, respectively. The asterisk indicates the Ape1 complex. Scale bar represents 200 nm.

(D) Localization of Ty1 VLPs and the Ape1 complex in prApe1-overexpressing cells. Cells overexpressing GFP-Ty1 Gag and prApe1 were treated with rapamycin for 6 hr. Scale bar represents 2 μm.

(E) Electron microscopic image of Ty1 VLPs and the Ape1 complex in prApe1-overexpressing cells. Cells used in (D) were treated with rapamycin for 5 hr. The arrow and asterisk indicate a cluster of Ty1 VLPs and the Ape1 complex, respectively. Scale bar represents 500 nm. See also Figures S1–S4.

mRNAs in a cytoplasmic dot-like structure (Checkley et al., 2010).

The surrounding particles in the Cvt complex seem to morphologically resemble Ty1 VLPs via electron microscopy. Initially, we used *atg1*Δ cells for electron microscopy because a defect in these cells prevents Cvt complex transport to the vacuole and thus the markedly enlarged Cvt complex remains outside the vacuole. Endogenous Ty1 Gag was specifically detected with anti-Ty1 Gag antibodies by immunoblot analysis (see Figure S1 available online). The surrounding particles of the Cvt complex were labeled with these antibodies under an electron microscope (Figure 1A and Figure S2). Because overexpression of the first 360 residues of Ty1 Gag has been shown to be sufficient for VLP formation (Brookman et al., 1995; Burns et al., 1992; Martin-Rendon et al., 1996), we monitored the behavior of Ty1 VLPs using ectopically overexpressed N-terminally GFP-tagged Ty1 Gag-p45 (residues 1–401) and p49 (residues 1–440). Because both proteins showed similar dot-like patterns next to the vacuole (Figure 1B and Figure S3), we used GFP-Ty1 Gag-p45 as a marker of the Ty1 VLP (GFP-Ty1 Gag). Using fluorescence microscopy, we found that the Ape1 complex, labeled with mRFP-prApe1, and GFP-Ty1 Gag were very closely localized as distinct dots adjacent to the vacuole (Figure 1B). Electron microscopy showed that GFP-Ty1 Gag was able to form VLPs, which localized next to the Ape1 complex (Figure 1C and Figure S4A). The overexpression of prApe1 resulted in enlargement of the Ape1 complex, which appeared as a large spherical structure that could be visualized by light microscopy (unpublished data). GFP-Ty1 Gag was localized adjacent to, but apparently distinct from, the Ape1 complex (Figures 1D and 1E and Figure S4B).

Ty1 VLPs Are Selective Cargo of Autophagosomes

Under autophagy-inducing conditions, we found that a substantial population of GFP-Ty1 Gag was transported to the vacuolar lumen (Figure 2A), suggesting that GFP-Ty1 Gag is delivered to the vacuole via autophagy. In the vacuole, disintegration of autophagic bodies, formed by the fusion of autophagosomes with the vacuole, is inhibited in *pep4*Δ cells (Takeshige et al., 1992). We found endogenous Ty1 VLPs inside autophagic bodies in *pep4*Δ cells (Figure 2B and Figure S5). GFP-Ty1 Gag, which is transported to the vacuole, is degraded by vacuolar hydrolases. As the GFP moiety is relatively stable in the vacuole, we monitored the transport of GFP-Ty1 Gag to the vacuole via the emergence of free GFP by immunoblot analysis (Suzuki et al., 2002). During autophagy, free GFP derived from GFP-Ty1 Gag was detected in wild-type cells; however, it was not seen in *atg1*Δ and *atg7*Δ cells (Figure 2C and Figure S6). Furthermore, because free GFP did not emerge in *pep4*Δ cells,

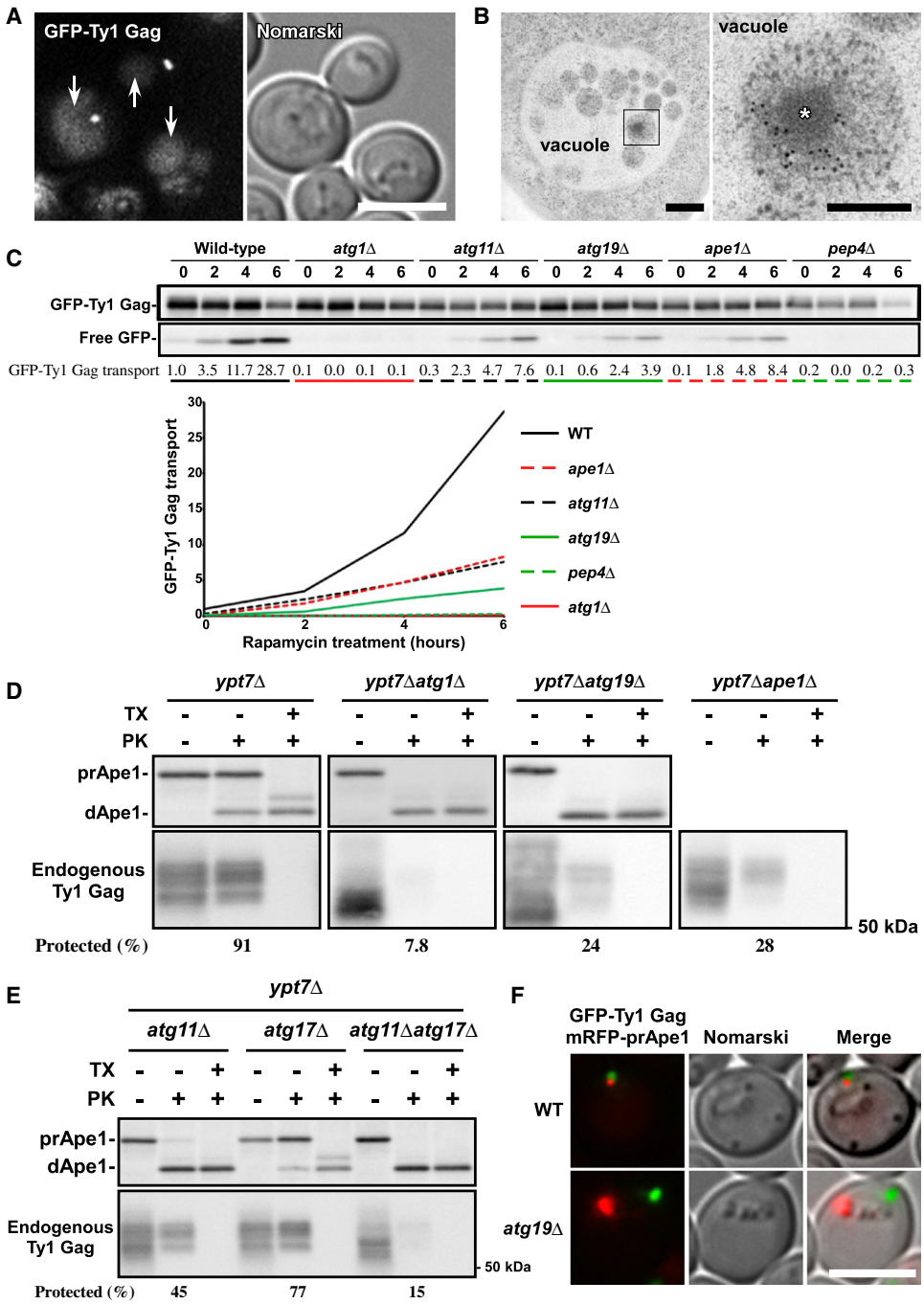

Figure 2. Ty1 VLPs Are Selective Cargo of Autophagosomes

(A) Ty1 Gag is transported to the vacuole. Cells overexpressing GFP-Ty1 Gag were treated with rapamycin for 6 hr. Arrows indicate vacuoles. Scale bar represents 5 μm.

(B) Immunoelectron microscopy with anti-Ty1 Gag antibodies. Endogenous Ty1 VLPs in autophagic bodies are recognized. *pep4*Δ cells were treated with rapamycin for 3 hr. The square in the left panel indicates the area shown in the right panel. An asterisk indicates the Ape1 complex. Scale bars represent 500 nm (left) and 200 nm (right), respectively.

(C) GFP-Ty1 Gag is transported to the vacuole by autophagy. Cells overexpressing GFP-Ty1 Gag were treated with rapamycin for the indicated hours. The levels of GFP-Ty1 Gag transport are estimated by dividing the density of free GFP by that of GFP-Ty1 Gag and normalized to the value of wild-type cells at 0 hr (numbers are shown below the immunoblot data).

(D and E) Endogenous Ty1 VLP is selectively enclosed in autophagosomes. Cells were incubated in a nitrogen starvation medium for 4.5 hr. Cell lysates were incubated on ice for 30 min in the presence of 1% Triton X-100 (TX) and/or 1 mg/ml proteinase K (PK). Reactions were terminated by the addition of 20% trichloroacetic acid. prApe1 and dApe1 indicate precursor Ape1 and degraded Ape1, respectively. Percentages of protected Ty1 Gag are calculated from the values obtained by densitometry.

cleavage of GFP-Ty1 Gag occurred inside the vacuole (Figure 2C). These results clearly show that the Ty1 VLP was transported to the vacuole via autophagy.

Next, we estimated how efficiently endogenous Ty1 VLPs were enclosed in autophagosomes via proteinase K protection assays. In *ypt7*Δ cells, autophagosomes accumulate in the cytoplasm because of a defect in vacuole fusion (Kirisako et al., 1999). In these cells, Ape1 was detected as a precursor (TX –, PK – in Figure 2D) but prApe1 outside autophagosomes were converted to degraded Ape1 (dApe1) by proteinase K treatment (TX –, PK + in Figure 2D). All prApe1 was converted to dApe1 by disintegrating autophagosomes through detergent treatment (TX +, PK + in Figure 2D). Proteinase K protection assays showed that about half of prApe1 was inside autophagosomes in *ypt7*Δ cells as previously reported (Ishihara et al., 2001), whereas the majority of Ty1 Gag was inside autophagosomes (Figure 2D). In *ypt7*Δ*atg1*Δ cells, neither prApe1 nor Ty1 Gag was protected (Figure 2D). These results indicate that Ty1 VLPs are enclosed into autophagosomes more efficiently than prApe1. We note that Ty1 Gag in the mock-treated control was found as lower molecular weight bands in *ypt7*Δ*atg1*Δ cells (Figure 2D). Indeed, we found that the Ty1 Gag patterns were similar between *ypt7*Δ and *ypt7*Δ*atg1*Δ lysates before the 30 min incubation on ice for the proteinase K protection assay (data not shown); thus, the differences in electrophoretic patterns might be caused by nonspecific degradation of Ty1 Gag outside autophagosomes during the incubation on ice.

We next investigated the mechanism by which Ty1 VLPs are selectively enclosed by autophagosomes. Atg11 and Atg19 are important for the selective engulfment of prApe1 by autophagosomes (Scott et al., 2001; Shintani et al., 2002). GFP cleavage assays showed that Ty1 transport was defective in *atg11*Δ, *atg19*Δ, and *ape1*Δ cells (Figure 2C). Proteinase K protection assays showed that the majority of prApe1 was outside autophagosomes in *ypt7*Δ*atg11*Δ and *ypt7*Δ*atg19*Δ cells, and consistently, that the level of endogenous Ty1 Gag enclosed in autophagosomes decreased in these strains (Figures 2D and 2E). These results show that Atg11, Atg19, and prApe1 are important for the selective enclosure of Ty1 VLPs into autophagosomes. Selective transport of α-mannosidase (Ams1) also requires these proteins (Shintani et al., 2002), suggesting a pivotal role of the Ape1 complex in Atg19-dependent selective autophagy. In *ypt7*Δ*atg17*Δ cells, enclosure of Ty1 VLPs into autophagosomes was slightly defective, whereas no Ty1 Gag was protected in *ypt7*Δ*atg11*Δ*atg17*Δ cells (Figure 2E). These results suggest that Atg17 plays a minor role in the selective enclosure of Ty1 VLPs into autophagosomes. We recently identified Atg34 as a receptor for selective autophagy (Suzuki et al., 2010; Watanabe et al., 2010); however, Atg34 was not involved in the selective transport of Ty1 VLPs (Figure S6).

In wild-type cells, GFP-Ty1 Gag was localized in the immediate vicinity of the Ape1 complex (94.9% of dots were associated, n = 54); however, only 13.5% (n = 58) of GFP-Ty1 Gag was associated with the Ape1 complex in *atg19*Δ cells (Figure 2F). We note that GFP-Ty1 Gag was not dispersed throughout the cytoplasm in the absence of Atg19 (Figure 2F); this indicates that Atg19 is not involved in Ty1 VLP cluster formation. It is therefore likely that Atg19 facilitates the association of Ty1 VLPs with the Ape1 complex.

The Atg19 N-Terminal Domain Is Specifically Required for Selective Transport of Ty1 VLPs

Atg19 acts as a receptor by linking cargo proteins to the pre-autophagosomal structure, the center of autophagosome formation (Figure 3A) (Shintani et al., 2002; Suzuki et al., 2001, 2002). Atg19 has a structurally stable domain at the N terminus (residues 1–123) (Watanabe et al., 2010). We found that the expression of Atg19 lacking this N-terminal domain ($Atg19^{\Delta 2-123}$) was comparable to that of full-length Atg19 (Figure S7A). Furthermore, $Atg19^{\Delta 2-123}$ cells exhibited normal transport of Ape1 and Ams1 (Figure 3B and Figure S7B) (Watanabe et al., 2010); however, these cells were defective in Ty1 Gag transport (Figure 3C). A proteinase K protection assay shows that Ty1 Gag was not engulfed by autophagosomes in $Atg19^{\Delta 2-123}$ cells although the majority of $Atg19^{\Delta 2-123}$ was protected like full-length Atg19 (Figure 3D).

We analyzed the physical interaction of Atg19 with GFP-Ty1 Gag. We found that endogenous Ty1 Gag was coprecipitated with GFP-Ty1 Gag (Figure 3E), suggesting that GFP-Ty1 Gag assembles into VLPs together with endogenous Ty1 Gag. Moreover, Atg19 was coprecipitated with GFP-Ty1 Gag (Figure 3E) but prApe1 was not (data not shown). We also observed that $Atg19^{1-123}$, $Atg19^{\Delta 2-123}$, and Atg19 lacking the Ams1- and prApe1-binding domains ($Atg19^{\Delta 153-362}$) (Shintani et al., 2002; Watanabe et al., 2010) still bound to GFP-Ty1 Gag (Figure 3E). Together, we conclude that residues 1–123 of Atg19 are specifically required for selective autophagy of Ty1 VLPs, although Atg19 is able to interact with Ty1 Gag without this region.

Selective Autophagy Regulates Retrotransposition Caused by Ty1 Elements under Nitrogen Starvation Conditions

Here we show that autophagy selectively delivers Ty1 VLPs to the vacuole; thus, we hypothesize that selective autophagy affects Ty1 transposition frequency. Because the transposition frequency of Ty1 elements at 20°C is approximately 60- to 100-fold higher than that at 30°C (Boeke et al., 1986; Paquin and Williamson, 1984), we quantified the Ty1 transposition frequency at 20°C. We examined the transport of Ty1 VLPs at 20°C and found that at this temperature Ty1 VLPs are also selectively targeted to autophagosomes by an Atg19-dependent mechanism (Figures 4A–4C).

The transposition frequencies under nutrient-replete conditions in wild-type, *atg1*Δ, and *atg19*Δ cells, estimated by the Ty1*his3-AI* mobility assay (Mou et al., 2006), were not significantly different (Figure S8). Next, we quantified the transposition frequency under nitrogen starvation conditions. In wild-type cells, the level of transposition frequency was basically unchanged during prolonged periods of starvation (Figure 4D). In contrast, the transposition frequency continually increased during starvation in *atg1*Δ and *atg19*Δ cells (Figure 4D). Taken together, we conclude that selective autophagy downregulates

(F) Localization of Ty1 VLPs and the Ape1 complex in wild-type and *atg19*Δ cells. Cells overexpressing GFP-Ty1 Gag were treated with rapamycin for 6 hr. See also Figure S5 and Figure S6.

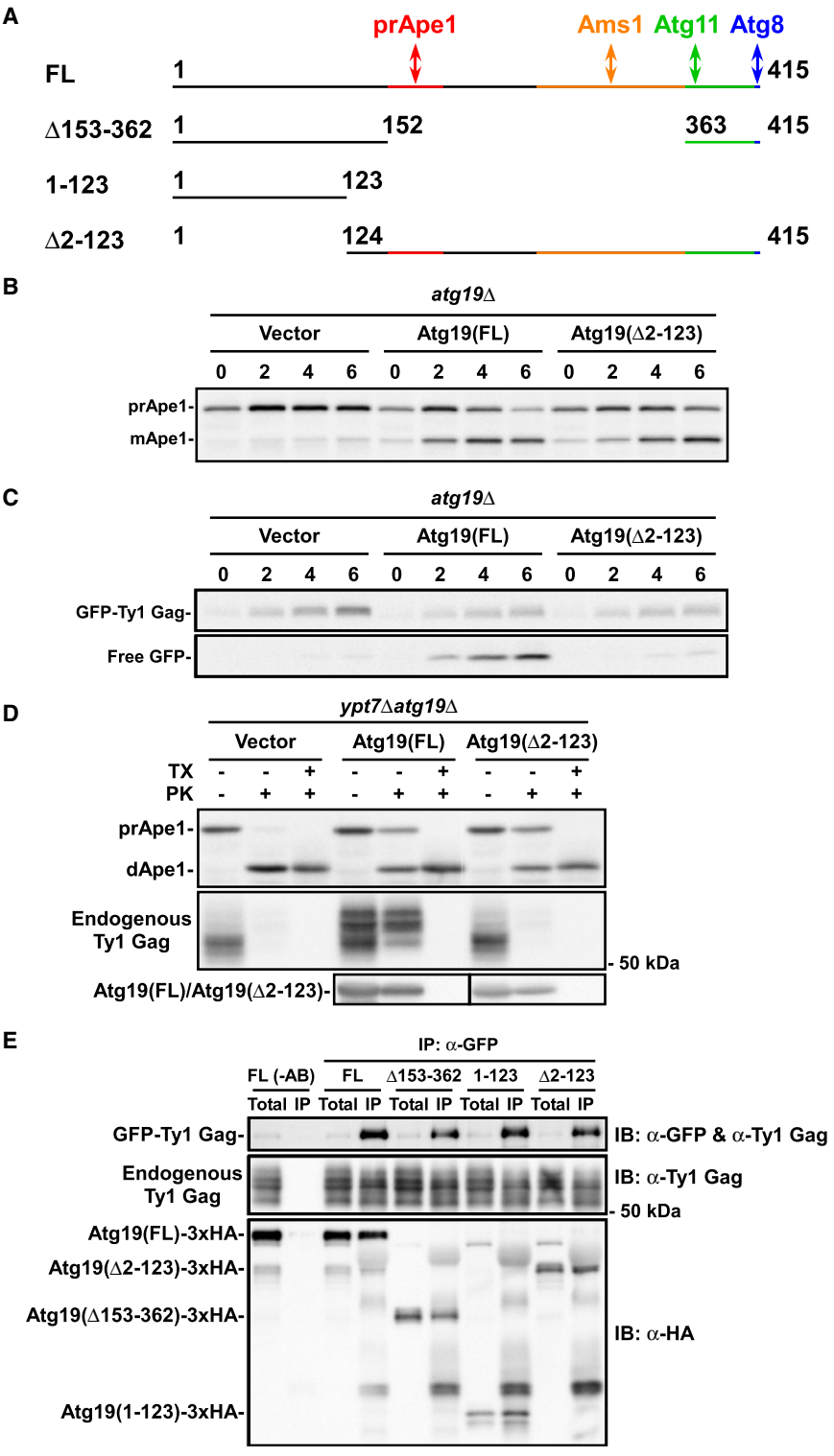

Figure 3. The Atg19 N-Terminal Domain Is Specifically Required for the Selective Transport of Ty1 VLPs

(A) Schematic diagram of the binding domains in Atg19. Atg19 interacts with prApe1, Ams1, Atg11, and Atg8 using distinct domains. FL indicates full-length.

(B) Atg19$^{\Delta 2-123}$ cells exhibit normal Ape1 transport. *atg19*Δ cells harboring the indicated plasmids were treated with rapamycin for the indicated number of hours. mApe1 indicates mature Ape1.

(C) Atg19$^{\Delta 2-123}$ cells are defective in Ty1 VLP transport. *atg19*Δ cells harboring GFP-Ty1 Gag and indicated plasmids were treated with rapamycin for the indicated hours.

(D) The engulfment of endogenous Ty1 VLPs by autophagosomes is defective in *atg19*$^{\Delta 2-123}$ cells. *ypt7*Δ*atg19*Δ cells harboring the indicated plasmids were subjected to the proteinase K protection assay.

(E) Physical interaction of Atg19 with Ty1 Gag. GFP-Ty1 Gag was overexpressed in *atg1*Δ*atg19*Δ cells and immunoprecipitated with an anti-GFP antiserum and probed with the indicated antibodies. See also Figure S7.

Ty1 retrotransposition during lengthy starvation in a manner that is dependent on Atg19.

We show that the Ty1 VLPs are selective cargo of autophagosomes and that Atg19 is responsible for this selectivity through engagement of the Cvt complex (Figure 4E). A genome-wide screen identified that the *atg17*Δ strain shows a decrease in Ty1 transposition under nutrient-replete conditions (Griffith et al., 2003). Because the defect in selective autophagy of Ty1 VLPs has little effect on Ty1 transposition under nutrient-replete conditions (Figure S8), we think that this phenotype might be an indirect effect as a result by the absence of *ATG17*. It is likely that the loading capacity of Cvt vesicles is too small to affect Ty1 transposition.

Transposable elements found in the genomes of almost all organisms act to introduce mutations in the host genome; this serves to generate a reservoir for new cellular regulation and function that may allow adaptation to various environmental conditions by modulating gene expression (Gogvadze and Buzdin, 2009; Volff, 2006). On the other hand, transposable elements may introduce disadvantageous or fatal mutations in the host genome. Here, we show that Ty1 transposition is downregulated by selective autophagy, which may serve to protect the yeast genome from excessive insertional mutagenesis under nutrient-limited conditions, a circumstance that cells are frequently faced with in natural environments.

In higher eukaryotes, p62 acts as a receptor for autophagosomes (Ichimura et al., 2008). A recent study has shown that p62 interacts with a capsid protein of the Sindbis virus, targeting

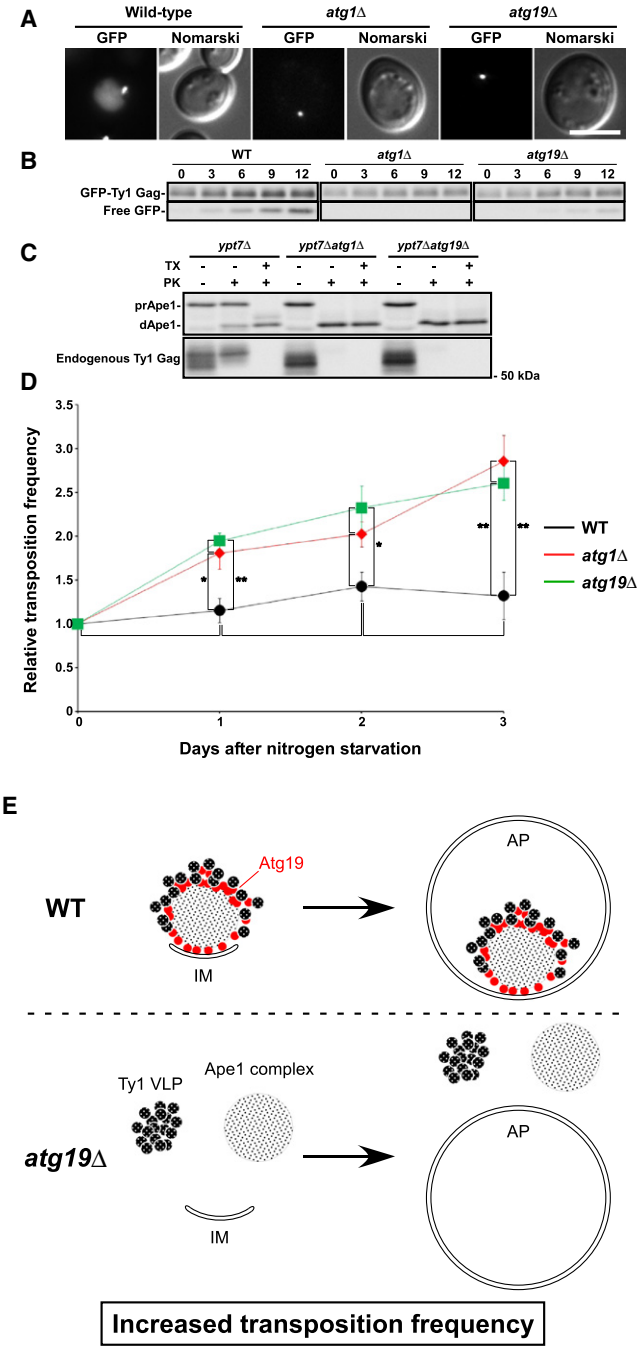

Figure 4. Selective Autophagy Regulates Retrotransposition Caused by Ty1 Elements under Nitrogen Starvation Conditions

(A) Localization of Ty1 Gag at 20°C. Cells overexpressing GFP-Ty1 Gag were treated with rapamycin for 12 hr at 20°C. In wild-type cells, the vacuole was stained with GFP but there was no staining in *atg1*Δ or *atg19*Δ cells. Scale bar represents 5 μm.

(B) GFP-Ty1 Gag is transported to the vacuole by selective autophagy at 20°C. Cells overexpressing GFP-Ty1 Gag were treated with rapamycin for the indicated hours at 20°C.

(C) Endogenous Ty1 VLP is selectively enclosed in autophagosomes at 20°C in an Atg19-dependent manner. Cells were incubated in a nitrogen starvation medium for 6 hr and subjected to the proteinase K protection assay.

(D) BY4741 cells harboring the Ty1*his3-AI* element (JC3212) were subjected to the Ty1*his3-AI* mobility assay (Mou et al., 2006). JC3212 background cells were transferred to a nitrogen starvation medium and collected on the indicated days. Error bars indicate standard errors. *$p < 0.05$; **$p < 0.01$; unlabeled lines indicate $p > 0.05$ (two-tailed Student's t test).

(E) Schematic diagram of Ty1 VLP transport. In wild-type cells, Atg19 acts to assemble the Cvt complex and mediates targeting of the Cvt complex to the isolation membrane (IM), the autophagosome precursor. Thus, the Cvt complex is selectively enclosed in autophagosomes. In the absence of Atg19, the Ty1 VLP cluster, the Ape1 complex, and autophagosomes are independently formed. See also Figure S8.

virus particles to autophagosomes for degradation (Orvedahl et al., 2010). Selective autophagy of the Ty1 VLP in yeast may be useful as a model system to study the elimination of virus particles from the cytoplasm of higher eukaryotes. The regulation of transposable element activities by selective autophagy may contribute to maintain genome integrity in eukaryotes. Further studies will uncover the physiological significance of selective autophagy in various species of eukaryotes.

EXPERIMENTAL PROCEDURES

Yeast Strains and Growth Conditions

The yeast strains used in this study are listed in the Supplemental Experimental Procedures. Standard protocols were used for yeast manipulation (Adams et al., 1998). The mRFP-Ape1 strain (GYS638) was constructed as previously described (Strømhaug et al., 2004). Cells were grown in either YEPD (1% yeast extract, 2% bacto-peptone, and 2% glucose) or SD + casamino acid (SDCA; 0.17% yeast nitrogen base w/o amino acids and ammonium sulfate, 1% casamino acid, 0.5% ammonium sulfate, and 2% glucose) medium with the appropriate supplements. To induce the *CUP1* promoter, cells were cultured for 1 day in medium containing 250 μM $CuSO_4$. Autophagy was induced by the addition of 0.4 μg/ml rapamycin (Sigma) or by shifting to a nitrogen starvation medium (SD(−N); 0.17% yeast nitrogen base without amino acids and ammonium sulfate, and 2% glucose). Cells were cultured at 30°C unless otherwise noted.

Plasmids

The plasmids used in this study are listed in the Supplemental Experimental Procedures. To construct pYEX-BX[GFP-Ty1 Gag-p49], the sequence of enhanced yeast green fluorescent protein (EYGFP) was cloned into the EcoRI-BamHI site of the pYEX-BX plasmid (Clontech). Subsequently, the *TYA* sequence of *YGRWTy1-1* was cloned into the plasmid, which resulted from digestion with BamHI, to generate pYEX-BX[GFP-Ty1 Gag-p49]. The pYEX-BX[GFP-Ty1 Gag-p45] plasmid was generated by deleting the 3′-terminal region of the *TyA* open reading frame by site-directed mutagenesis. The *Hind*III-*Xba*I fragment of pYEX-BX[GFP-Ty1 Gag-p49] was cloned into pRS424 to generate pRS424[GFP-Ty1 Gag-p45]. Atg19 with its natural promoter was cloned into pRS426 to generate pRS426[Atg19], and the BamHI site was introduced immediately before the stop codon by site-directed mutagenesis. The 3× haemagglutinin (HA) sequence was excised from the 008-NHA-316 plasmid (Laboratory stock) with BglII and cloned into this plasmid to produce pRS424[Atg19-3xHA]. $Atg19^{\Delta 2-123}$, $Atg19^{\Delta 153-362}$, and $Atg19^{1-123}$ were generated by site-directed mutagenesis.

Electron Microscopy

Electron microscopy was performed by Tokai-EMA (Nagoya, Japan) as described previously (Okamoto et al., 2009). Briefly, cells were harvested by centrifugation and the medium was removed by aspiration. The pellets were sandwiched with copper grids and rapidly frozen in liquid propane using Leica EM CPC (Leica). The cells were freeze-substituted in 2% osmium tetroxide dissolved in acetone for ultrastructural analysis or in acetone containing 1%−3% distilled water for immunoelectron microscopy. Samples were embedded in Quetol 651 or LR White resin. Anti-Ty1 Gag antibodies (Diagenode anti-Ty1-tag) and anti-Ape1 antiserum (Suzuki et al., 2002) were used to detect Ty1 VLPs and the Ape1 complex, respectively.

Fluorescence Microscopy

Fluorescence microscopy was performed using a TIR-FM system (Olympus) equipped with a UPlanSApo 100× Oil (NA: 1.40) and a CoolSNAP HQ CCD camera (Nippon Roper) as described (Suzuki et al., 2010). Blue (Sapphire 488-20, Coherent) and yellow lasers (85-YCA-010, Melles Griot) were used for excitation of GFP and mRFP, respectively. Images were acquired using MetaMorph software (Molecular Devices).

Immunoblot Analysis

Cell lysates were prepared by the alkaline lysis method or by glass bead disruption (Horvath and Riezman, 1994; Suzuki et al., 2004). Anti-GFP antibodies (Roche, 1814460), anti-Ape1p antiserum, anti-Ty1 Gag antibodies raised against the Glu-Val-His-Thr-Asn-Gln-Asp-Pro-Leu-Asp peptide (Bastin et al., 1996) (Diagenode, anti-Ty1-tag) and anti-HA antibodies (Covance, MMS-101R [16B12]; Roche, 1867423 [3F10]) were used as primary antibodies. Horseradish peroxidase-conjugated antibodies (Jackson ImmunoResearch) were used as secondary antibodies. Chemiluminescence signals produced by an ECL reagent (Perkin-Elmer, Western Lightning Plus-ECL; Wako, ImmunoStar LD) were detected using a CCD camera system (Fujifilm, LAS4000).

Immunoprecipitation experiments were performed as previously described (Suzuki et al., 2007). GFP-Ty1 Gag was immunoprecipitated with an anti-GFP antiserum (Invitrogen, A6455), and detected with a mixture of anti-GFP antibodies (Roche, 1814460) and anti-Ty1 Gag antibodies. Endogenous Ty1 Gag was detected with anti-Ty1 Gag antibodies. Atg19 variants tagged with HA were probed with anti-HA antibodies (Covance, MMS-101R [16B12]) and detected using ExactaCruz B (Santa Cruz Biotechnology, sc-45039).

Proteinase K Protection Assay

Cells were grown to a density of approximately OD_{600} = 1.5 and incubated for 4.5 hr in SD(−N) medium. Collected cells were converted to spheroplasts and mechanically disrupted with 3.0-μm polycarbonate filters (Whatman, 110612) in lysis buffer ($HES_{1.0}$ buffer; 20 mM HEPES pH 7.5, 5 mM EDTA, and 1 M sorbitol). After cell debris was removed by centrifugation, cell lysates were divided into aliquots and treated with or without 1% Triton X-100 (Nacalai Tesque, 35501-15) and proteinase K (Roche, 3115879) for 30 min on ice. The reactions were terminated by addition of 20% trichloroacetic acid. Precipitants were washed with acetone and dissolved in SDS-PAGE sample buffer containing 4 mM Pefabloc SC (Roche, 11429876001). Equivalent protein amounts were subjected to immunoblot analysis.

Ty1*his3-AI* Mobility Assay

The Ty1*his3-AI* mobility assay was performed as previously described (Mou et al., 2006) with modification. Briefly, cells were cultured in YEPD medium in flasks with vigorous shaking at 20°C for 4 days. Saturated cultures were diluted to a density of approximately OD_{600} = 0.3 and grown to approximately OD_{600} = 1.5. Cells were transferred to SD(−N) medium and incubated at 20°C. Aliquots of each culture were plated onto YEPD and SC(−His) plates. The frequency of Ty1*his3-AI* transposition was estimated by the number of His+ cells divided by the number of viable cells in the same culture volume. The number of colonies was counted after incubation for 7 days at 30°C. The relative transposition frequency was calculated by dividing transposition frequency at the indicated time by the frequency at day 0 for each strain.

SUPPLEMENTAL INFORMATION

Supplemental Information includes eight figures and Supplemental Experimental Procedures and can be found with this article online at doi:10.1016/j.devcel.2011.06.023.

ACKNOWLEDGMENTS

We thank Drs. M. Joan Curcio, David J. Garfinkel, Jef D. Boeke, and Daniel J. Klionsky for strains and materials. We thank Dr. Tomoko Andoh for helpful discussion on the experiments. We also thank the National Institute for Basic Biology (NIBB) Center for Analytical Instruments for their technical assistance. This work was supported by Grants-in-Aids for Scientific Research from the Ministry of Education, Culture, Sports, Science and Technology of Japan.

Received: November 12, 2010
Revised: April 18, 2011
Accepted: June 17, 2011
Published online: August 15, 2011

REFERENCES

Adams, A., Gottschling, D.E., Kaiser, C.A., and Stearns, T. (1998). Methods in Yeast Genetics, 1997 Edition (Cold Spring Harbor, NY: Cold Spring Harbor Laboratory Press).

Baba, M., Osumi, M., Scott, S.V., Klionsky, D.J., and Ohsumi, Y. (1997). Two distinct pathways for targeting proteins from the cytoplasm to the vacuole/lysosome. J. Cell Biol. *139*, 1687–1695.

Bastin, P., Bagherzadeh, Z., Matthews, K.R., and Gull, K. (1996). A novel epitope tag system to study protein targeting and organelle biogenesis in Trypanosoma brucei. Mol. Biochem. Parasitol. *77*, 235–239.

Boeke, J.D., Styles, C.A., and Fink, G.R. (1986). *Saccharomyces cerevisiae SPT3* gene is required for transposition and transpositional recombination of chromosomal Ty elements. Mol. Cell. Biol. *6*, 3575–3581.

Brookman, J.L., Stott, A.J., Cheeseman, P.J., Adamson, C.S., Holmes, D., Cole, J., and Burns, N.R. (1995). Analysis of TYA protein regions necessary for formation of the Ty1 virus-like particle structure. Virology *212*, 69–76.

Burns, N.R., Saibil, H.R., White, N.S., Pardon, J.F., Timmins, P.A., Richardson, S.M., Richards, B.M., Adams, S.E., Kingsman, S.M., and Kingsman, A.J. (1992). Symmetry, flexibility and permeability in the structure of yeast retrotransposon virus-like particles. EMBO J. *11*, 1155–1164.

Checkley, M.A., Nagashima, K., Lockett, S.J., Nyswaner, K.M., and Garfinkel, D.J. (2010). P-body components are required for Ty1 retrotransposition during assembly of retrotransposition-competent virus-like particles. Mol. Cell. Biol. *30*, 382–398.

Feschotte, C., Jiang, N., and Wessler, S.R. (2002). Plant transposable elements: where genetics meets genomics. Nat. Rev. Genet. *3*, 329–341.

Garfinkel, D.J., Boeke, J.D., and Fink, G.R. (1985). Ty element transposition: reverse transcriptase and virus-like particles. Cell *42*, 507–517.

Gogvadze, E., and Buzdin, A. (2009). Retroelements and their impact on genome evolution and functioning. Cell. Mol. Life Sci. *66*, 3727–3742.

Griffith, J.L., Coleman, L.E., Raymond, A.S., Goodson, S.G., Pittard, W.S., Tsui, C., and Devine, S.E. (2003). Functional genomics reveals relationships between the retrovirus-like Ty1 element and its host *Saccharomyces cerevisiae*. Genetics *164*, 867–879.

Horvath, A., and Riezman, H. (1994). Rapid protein extraction from *Saccharomyces cerevisiae*. Yeast *10*, 1305–1310.

Ichimura, Y., Kumanomidou, T., Sou, Y.S., Mizushima, T., Ezaki, J., Ueno, T., Kominami, E., Yamane, T., Tanaka, K., and Komatsu, M. (2008). Structural basis for sorting mechanism of p62 in selective autophagy. J. Biol. Chem. *283*, 22847–22857.

Ishihara, N., Hamasaki, M., Yokota, S., Suzuki, K., Kamada, Y., Kihara, A., Yoshimori, T., Noda, T., and Ohsumi, Y. (2001). Autophagosome requires specific early Sec proteins for its formation and NSF/SNARE for vacuolar fusion. Mol. Biol. Cell *12*, 3690–3702.

Kirisako, T., Baba, M., Ishihara, N., Miyazawa, K., Ohsumi, M., Yoshimori, T., Noda, T., and Ohsumi, Y. (1999). Formation process of autophagosome is traced with Apg8/Aut7p in yeast. J. Cell Biol. *147*, 435–446.

Klionsky, D.J., Cueva, R., and Yaver, D.S. (1992). Aminopeptidase I of *Saccharomyces cerevisiae* is localized to the vacuole independent of the secretory pathway. J. Cell Biol. *119*, 287–299.

Lander, E.S., Linton, L.M., Birren, B., Nusbaum, C., Zody, M.C., Baldwin, J., Devon, K., Dewar, K., Doyle, M., FitzHugh, W., et al; International Human Genome Sequencing Consortium. (2001). Initial sequencing and analysis of the human genome. Nature *409*, 860–921.

Martin-Rendon, E., Marfany, G., Wilson, S., Ferguson, D.J., Kingsman, S.M., and Kingsman, A.J. (1996). Structural determinants within the subunit protein of Ty1 virus-like particles. Mol. Microbiol. *22*, 667–679.

Merkulov, G.V., Swiderek, K.M., Brachmann, C.B., and Boeke, J.D. (1996). A critical proteolytic cleavage site near the C terminus of the yeast retrotransposon Ty1 Gag protein. J. Virol. *70*, 5548–5556.

Mou, Z., Kenny, A.E., and Curcio, M.J. (2006). Hos2 and Set3 promote integration of Ty1 retrotransposons at tRNA genes in *Saccharomyces cerevisiae*. Genetics *172*, 2157–2167.

Okamoto, K., Kondo-Okamoto, N., and Ohsumi, Y. (2009). Mitochondria-anchored receptor Atg32 mediates degradation of mitochondria via selective autophagy. Dev. Cell *17*, 87–97.

Onodera, J., and Ohsumi, Y. (2005). Autophagy is required for maintenance of amino acid levels and protein synthesis under nitrogen starvation. J. Biol. Chem. *280*, 31582–31586.

Orvedahl, A., MacPherson, S., Sumpter, R., Jr., Tallóczy, Z., Zou, Z., and Levine, B. (2010). Autophagy protects against Sindbis virus infection of the central nervous system. Cell Host Microbe *7*, 115–127.

Paquin, C.E., and Williamson, V.M. (1984). Temperature effects on the rate of ty transposition. Science *226*, 53–55.

Scott, S.V., Guan, J., Hutchins, M.U., Kim, J., and Klionsky, D.J. (2001). Cvt19 is a receptor for the cytoplasm-to-vacuole targeting pathway. Mol. Cell *7*, 1131–1141.

Shintani, T., Huang, W.P., Stromhaug, P.E., and Klionsky, D.J. (2002). Mechanism of cargo selection in the cytoplasm to vacuole targeting pathway. Dev. Cell *3*, 825–837.

Strømhaug, P.E., Reggiori, F., Guan, J., Wang, C.W., and Klionsky, D.J. (2004). Atg21 is a phosphoinositide binding protein required for efficient lipidation and localization of Atg8 during uptake of aminopeptidase I by selective autophagy. Mol. Biol. Cell *15*, 3553–3566.

Suzuki, K., and Ohsumi, Y. (2007). Molecular machinery of autophagosome formation in yeast, *Saccharomyces cerevisiae*. FEBS Lett. *581*, 2156–2161.

Suzuki, K., Kirisako, T., Kamada, Y., Mizushima, N., Noda, T., and Ohsumi, Y. (2001). The pre-autophagosomal structure organized by concerted functions of *APG* genes is essential for autophagosome formation. EMBO J. *20*, 5971–5981.

Suzuki, K., Kamada, Y., and Ohsumi, Y. (2002). Studies of cargo delivery to the vacuole mediated by autophagosomes in *Saccharomyces cerevisiae*. Dev. Cell *3*, 815–824.

Suzuki, K., Noda, T., and Ohsumi, Y. (2004). Interrelationships among Atg proteins during autophagy in *Saccharomyces cerevisiae*. Yeast *21*, 1057–1065.

Suzuki, K., Kubota, Y., Sekito, T., and Ohsumi, Y. (2007). Hierarchy of Atg proteins in pre-autophagosomal structure organization. Genes Cells *12*, 209–218.

Suzuki, K., Kondo, C., Morimoto, M., and Ohsumi, Y. (2010). Selective transport of α-mannosidase by autophagic pathways: identification of a novel receptor, Atg34p. J. Biol. Chem. *285*, 30019–30025.

Takeshige, K., Baba, M., Tsuboi, S., Noda, T., and Ohsumi, Y. (1992). Autophagy in yeast demonstrated with proteinase-deficient mutants and conditions for its induction. J. Cell Biol. *119*, 301–311.

Volff, J.N. (2006). Turning junk into gold: domestication of transposable elements and the creation of new genes in eukaryotes. Bioessays *28*, 913–922.

Voytas, D., and Boeke, J.D. (2002). Ty1 and Ty5 of *Saccharomyces cerevisiae*. In Mobile DNA II, N.L. Craig, R. Craigie, M. Gellert, and A.M. Lambowitz, eds. (Washington, DC: ASM Press), pp. 631–661.

Watanabe, Y., Noda, N.N., Kumeta, H., Suzuki, K., Ohsumi, Y., and Inagaki, F. (2010). Selective transport of α-mannosidase by autophagic pathways: structural basis for cargo recognition by Atg19 and Atg34. J. Biol. Chem. *285*, 30026–30033.